LABORATORY SCIENCE

Mechanical outcome of accelerated corneal crosslinking evaluated by Brillouin microscopy

Joshua N. Webb, BS, Johnny P. Su, PhD, Giuliano Scarcelli, PhD

Purpose: To quantify corneal mechanical changes induced by corneal crosslinking (CXL) procedures of different ultraviolet-A (UVA) intensity and exposure time using Brillouin microscopy.

Settings: University of Maryland, College Park, Maryland, USA.

Design: Experimental study.

Methods: Porcine cornea samples were debrided of epithelia and soaked with riboflavin 0.1% solution. Samples were exposed to a standard 5.4 J/cm^2 of UVA radiation with varying intensity and exposure time as follows: 3 mW/cm^2 for 30.0 minutes, 9 mW/cm^2 for 10.0 minutes, 34 mW/cm^2 for 2.65 minutes, and 50 mW/cm^2 for 1.80 minutes. Using Brillouin microscopy, the Brillouin modulus for each sample was computed as a function of radiation intensity/exposure time. For validation, the Young's modulus was found with the stress–strain test and compared at each irradiation condition.

Results: The standard 3 mW/cm^2 irradiance condition produced a significantly larger increase in corneal Brillouin modulus than the 9 mW/cm^2 ($P \leq .05$), 34 mW/cm^2 ($P \leq .01$), and 50 mW/cm^2 ($P \leq .01$) conditions. Depth analysis showed similar anterior sections of the standard and 9 mW/cm^2 conditions but significantly less stiffening in the central and posterior of the 9 mW/cm^2 condition. The stiffening of the standard protocol was significantly larger in all sections of the 34 mW/cm^2 and 50 mW/cm^2 conditions ($P \leq .01$). The overall change in Brillouin-derived Brillouin modulus correlated with the increase in Young's modulus ($R^2 = 0.98$).

Conclusions: At a constant UVA light dose, accelerating the irradiation process decreased CXL stiffening. Brillouin analysis showed that accelerated protocols were especially ineffective in the deeper portions of the cornea.

J Cataract Refract Surg 2017; 43:1458–1463 © 2017 ASCRS and ESCRS

Corneal ectasia resulting from progressive keratoconus or refractive surgery can lead to progressive loss of vision and the need for corneal transplantation.[1,2] Clinically observed alterations in corneal morphology, a distinguishing characteristic of ectasia, are believed to be the consequence of a non-uniform decrease in stiffness of the corneal stroma.[3–6] To combat ectasia, the U.S. Food and Drug Administration recently approved corneal crosslinking (CXL). The accepted CXL procedure involves the debridement of the corneal epithelium followed by a 30-minute application of riboflavin solution (riboflavin 0.1%–dextran 20.0%) and an additional 30 minutes of ultraviolet-A (UVA) exposure (3 mW/cm^2; 5.4 J/cm^2). The photochemical reaction between the riboflavin photosensitizer and UVA light has been shown to increase the covalent bonding within the stroma, thereby increasing the overall stiffness of the cornea and halting ectasia.[7,8]

Recently, much effort has focused on decreasing the overall treatment time of the CXL procedure. It was proposed that treatment time could be shortened by increasing the radiation intensity because the biological effects should only depend on the total energy dose.[8,9] Although protocols using intensities up to 50 mW/cm^2 for less than 2 minutes of exposure time were suggested,[9] the evidence does not conclusively support accelerated CXL in clinical settings. Wernli et al.[10] reported a significant reduction in CXL stiffening when the procedure was performed above a 45 mW/cm^2 intensity. Hammer et al.[11] found a decrease in CXL effectiveness when comparing the standard protocol with a treatment using a radiation intensity of just 9 mW/cm^2. In addition, all previous mechanical studies observed the stiffness changes as a function of irradiance regime without spatial resolution.[10–12]

To assess the spatially varying effects of accelerated CXL, indirect techniques have been used; these include

Submitted: April 27, 2017 | Final revision submitted: June 26, 2017 | Accepted: July 29, 2017

From the Fischell Department of Bioengineering, University of Maryland, College Park, Maryland, USA.

Presented in part at the 18th International Congress on Wavefront & Presbyopic Refractive Corrections, San Jose, California, USA, February 2017.

Supported in part by the National Science Foundation (CMMI-1537027) and by the National Institutes of Health (K25EB015885).

Corresponding author: Giuliano Scarcelli, PhD, University of Maryland, 2218 Kim Engineering Building, College Park, Maryland 20742, USA. E-mail: scarc@umd.edu.

0886-3350/$ - see frontmatter
https://doi.org/10.1016/j.jcrs.2017.07.037

fluorescence imaging to assess riboflavin penetration[11] or optical coherence tomography to quantify the depth location of refractive index changes within the stroma (ie, the demarcation line).[9,13] We used recently developed Brillouin microscopy, which can directly assess corneal mechanics with 3-dimensional resolution to observe the depth dependence of stiffening after accelerated CXL protocols. As expected, we found the standard 3 mW/cm^2 radiation intensity for 30 minutes of exposure time produced the largest stiffness increase. Depth analysis showed that the 9 mW/cm^2 intensity condition could match the stiffening of the standard protocol in the anterior stroma but that it produced lower stiffening in the central and posterior sections.

MATERIALS AND METHODS

Corneal Crosslinking

Fresh porcine eyes were obtained from a local slaughterhouse (Frederick, Maryland, USA). For all eyes, the epithelium was carefully removed by scraping with a razor blade. The eyes were then dissected in order to punch two 5.0 mm corneal disk samples (Integra Miltex Disposable Biopsy Punch). Each disk sample was treated with 1 drop of riboflavin 0.1%–dextran 20.0% solution every 3 minutes for 30 minutes. After undergoing identical procedures, 1 of the 2 samples was set aside as the control while the other sample was exposed to UVA radiation. In all experimental settings, a constant UVA energy of 5.4 J/cm^2 was provided by a high-power UV Curing Light-Emitting Diode System (Thorlabs, Inc.). Four treatment regimens were performed. Table 1 shows the regimens.

Brillouin Microscopy

After the CXL procedure, the control disks and crosslinked corneal disks were imaged via Brillouin microscopy with a setup and procedures described previously.[14–17] Briefly, the confocal Brillouin microscope uses a 532 nm laser with an optical power of 10 mW. Light was focused into the sample by a ×20 objective lens with numerical aperture of 0.4 (Olympus America, Inc.) with transverse resolution of approximately 1 μm and depth resolution of approximately 4 μm. The scattered light, collected through the same objective, was coupled into a single mode fiber and delivered to a 2-stage VIPA spectrometer with an incorporated EMCCD camera (IXon Du-897, Andor Technology Ltd). Each Brillouin spectrum was acquired in 0.2 second. To quantify the Brillouin shift at each sample location, raw spectra from the camera were fitted using a Lorentzian function and calibrated using the known frequency shifts of water and glass.

From the Brillouin frequency shift, the local mechanical properties of the cornea can be estimated using the following relationship:

$$M' = \frac{\rho \nu_B^2 \lambda_i^2}{4n^2}$$

where M' is the longitudinal elastic modulus (refer to it here as the Brillouin modulus), ν_B is the measured Brillouin frequency shift, n is the refractive index of the material, λ_i is the wavelength of the incident photons, and ρ is the density of the material. The spatially varying ratio of ρ/n^2 was approximated to the constant value of 0.57 g/cm^3 based on literature values[16–21]; this was estimated to introduce a 0.3% uncertainty throughout the cornea.[22,23]

Table 1. Corneal crosslinking treatment regimen by group.

Group	Eyes	Irradiation Energy (J/cm^2)	Irradiation Intensity (mW/cm^2)	Irradiation Time (Min)
1	4	5.4	3	30.00
2	6	5.4	9	10.00
3	6	5.4	34	2.65
4	6	5.4	50	1.80

Brillouin Image Analysis

The corneal samples were set next to each other on the Brillouin microscope and imaged within the same acquisition run. Therefore, each scan imaged the frequency shift of both the control and crosslinked sample as a function of depth. For each scan, a depth cross-section (XZ) was collected, producing a 1000 μm (lateral) × 1400 μm (axial) image of Brillouin shift. A central sliver of each corneal cross-section was chosen for consistent post-processing analysis. In addition to the entire cornea sample, the cross-sections were divided into 3 equal segments (anterior, central, and posterior) for depth analysis. For this analysis, the depth of cornea (d) was normalized for each set of corneal samples to compare the Brillouin modulus of each sample in the anterior ($0 < d \leq 0.33$), central ($0.33 < d \leq 0.66$), and posterior ($0.66 < d \leq 1$) segment.

Compressive Biomechanical Testing

All samples were measured with compressive mechanical testing immediately after Brillouin imaging using a home-built compressive stress–strain instrument. The instrument consisted of a metallic baseplate topped with finely gritted sandpaper to prevent unwanted slippage and a downward-moving plunger containing a force-measuring loading cell (Futek Advanced Sensor Technology, Inc.) that is controlled via a motorized translational stage (Zaber Technologies, Inc.). Before every sample, the plunger was systematically moved downward until a reaction force from the baseplate was detected. The plunger position was then recorded and later used to calculate the total thickness of the sample.

The corneal sample was placed on the bottom plate of the instrument and the plunger compressed the sample at a constant downward rate of 10 μm/s. Using a purpose-designed Labview software program (National Instruments Corp.), the increasing compression force from the plunger and the corresponding material displacement were measured to produce the stress–strain curve of the material. The plunger position at which a reaction force was first sensed was noted in conjunction with the previously recorded baseplate position to accurately quantify the thickness of each sample. To obtain the Young's modulus of a sample, respective stress (force/area) versus strain (displacement/thickness) graphs were plotted and the slope of the linear segment of the curve following the sleek strain was quantified. Using the stress versus strain curve for each sample, the Young's modulus was reported by fitting the tangent line at 15% strain. A consistent 15% strain was chosen to observe the linear elastic behavior of the biological tissue as shown by Wernli et al.[10]

To compare with the compressive mechanical test, the Brillouin modulus was calculated from the Brillouin frequency shift and averaged the value over the whole sample. First, as for the traditional modulus analysis, the Brillouin modulus of CXL samples were compared with their respective nonirradiated controls.

Statistical Analysis

First, to characterize individual CXL protocols, a paired 2-tailed t test was performed by comparing CXL samples with their respective controls cut from the same eye. Then, to compare different irradiation conditions, the stiffening effects of CXL protocols were analyzed by comparing the percentage difference of both Brillouin and Young's moduli. The percentage difference for both the moduli were found per eye using the following equation: Modulus (X) Percentage Difference $= 100(X_{CXL} - X_{Control})/(X_{Control})$. The respective moduli percentage differences for the samples in each irradiation group were averaged $\pm$ SEM. A Wilcoxon rank-sum test was used to assess the significance in comparisons between

samples and/or corneal sections. A P value of 0.05 or less was considered statistically significant.

RESULTS

All CXL protocols produced a statistically significant increase in stiffness compared with nonirradiated control conditions ($P \leq .05$) A comparison of the mechanical outcome of the varying CXL procedures by quantifying the percentage change in Young's modulus with respect to each control found that the standard protocol, 3 mW/cm^2 of UVA power for 30 minutes was significantly more effective than the 34 mW/cm^2 ($P \leq .05$) and 50 mW/cm^2 ($P \leq .01$), the 9 mW/cm^2 condition was statistically significantly higher than the 50 mW/cm^2 ($P \leq .01$), and there was no significant difference between the 34 mW/cm^2 and 50 mW/cm^2 conditions. Figure 1 shows the average percentage change in Young's modulus ± SEM for the 4 irradiation conditions.

A comparison of the Brillouin modulus of CXL samples to their respective nonirradiated controls showed that all CXL protocols produced a statistically significant increase in corneal stiffness compared with their control ($P \leq .05$). Figure 2 shows the stiffness outcome of the CXL protocols as measured by Brillouin microscopy. Figure 2, *a*, shows the representative cross-sectional Brillouin images of corneas from each irradiation condition with the color encoding the Brillouin frequency shift at each location. Computation of the percentage change in the Brillouin modulus for each irradiation condition showed that the 3 mW/cm^2 CXL condition resulted in higher corneal stiffening than the 9 mW/cm^2 ($P \leq .05$), 34 mW/cm^2 ($P \leq .01$), and 50 mW/cm^2 ($P \leq .01$); the 9 mW/cm^2 had significantly higher stiffening than the 34 mW/cm^2 ($P \leq .01$) and 50 mW/cm^2 ($P \leq .01$), and the 34 mW/cm^2 and 50 mW/cm^2 irradiation conditions did not significantly differ in CXL-induced stiffening. Figure 2, *b*, shows the stiffening as a function of radiation intensity.

Figure 3 shows the relationship between Young's modulus and the average Brillouin modulus of the cornea sample. Each of the 4 points in Figure 3 represents the average of all the samples at a given irradiation condition. As radiation intensity decreased, both the Young's modulus percentage change and the Brillouin modulus percentage change increased at a similar rate. The similar rate of increase resulted in a highly statistically significant linear correlation between the percentage change of Young's modulus and the percentage change of the Brillouin modulus ($R^2 = 0.985$).

Figure 4 shows the percentage change in Brillouin modulus for each irradiance condition in the anterior, central, and posterior of the cornea. These findings were by obtained using Brillouin microscopy to perform a depth-dependent analysis on the corneas and calculate the percentage change in the Brillouin modulus in the anterior, central, and posterior sections of the cornea. There was no statistical significance in stiffening in the anterior section the 3 mW/cm^2 and 9 mW/cm^2 conditions. However, the difference between the 2

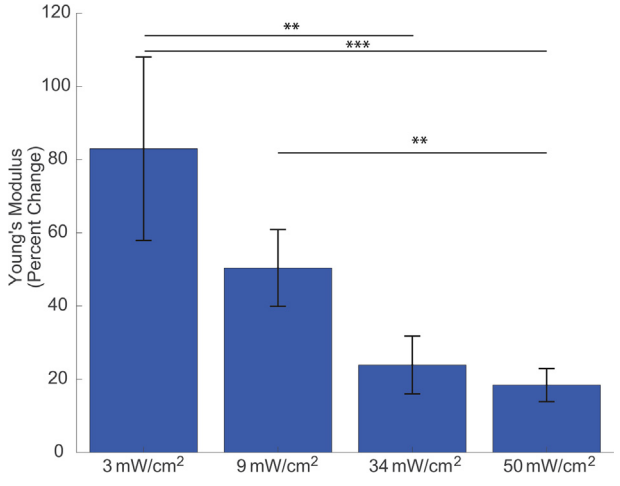

Figure 1. The averaged percentage change in Young's modulus for each irradiation condition from 3 to 50 mW/cm^2. As the intensity increases, the change in Young's modulus decreases. Error bars represent the SEM for each condition (** = $P < .01$; *** = $P < .001$).

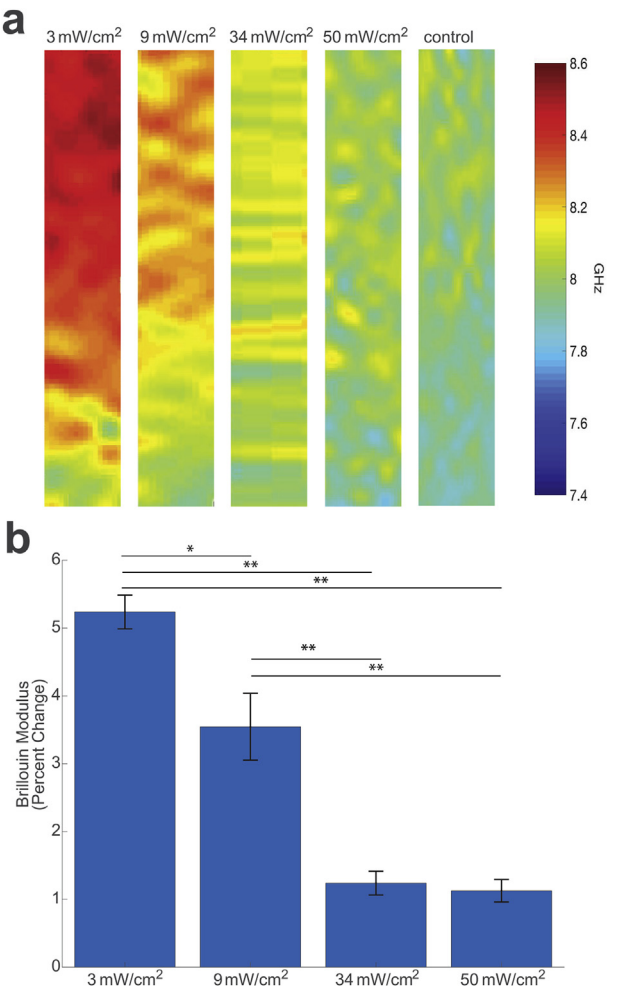

Figure 2. *a*: Representative image (700 μm × 100 μm) produced with Matlab software (*color map: jet*) of the Brillouin shifts for each condition. Because of the relationship between shift and Brillouin modulus, a higher Brillouin shift correlates to a higher Brillouin modulus. The corneal slices are positioned top down from the anterior to the posterior. *b*: The averaged percentage change in Brillouin modulus for each irradiation condition from 3 to 50 mW/cm^2. As the intensity increases, the overall change in Brillouin modulus decreases. Error bars represent the SEM for each condition (* = $P < .05$; ** = $P < .01$).

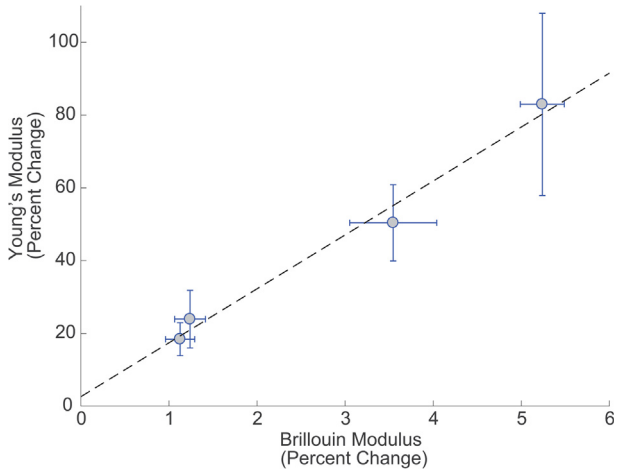

Figure 3. Correlation between percentage difference of mechanically yielded Young's modulus and Brillouin microscopy–derived Brillouin modulus. The corneas were exposed to a constant energy dose of 5.4 J/cm^2 at a variety of light intensities and exposure times: (*from left to right*) 50 mW/cm^2 for 1.80 minutes, 34 mW/cm^2 for 2.65 minutes, 9 mW/cm^2 for 10.0 minutes, 3 mW/cm^2 for 30.0 minutes. The correlation yielded a line of best fit of $y = 14.82 \times +2.605$ with a correlation coefficient of $R^2 = 0.9849$. Error bars represent the SEM for each condition.

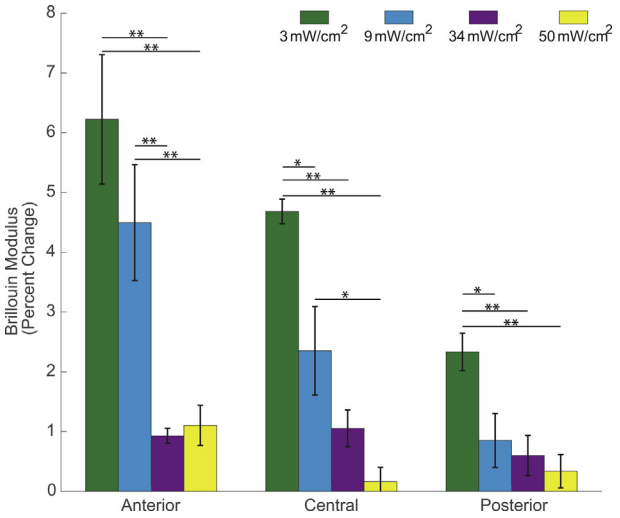

Figure 4. Brillouin modulus at a constant energy dose of 5.4 J/cm^2 as a function of radiation intensities and exposure times (*green*) 3 mW/cm^2 for 30.0 minutes, (*blue*) 9 mW/cm^2 for 10.0 minutes, (*purple*) 34 mW/cm^2 for 2.65 minutes, and (*yellow*) 50 mW/cm^2 for 1.80 minutes as well as corneal section (anterior, central, and posterior). Error bars represent the SEM for each condition (* = $P < .05$; ** = $P < .01$).

conditions was statistically significant in the central and posterior sections of the corneas ($P \leq .05$). In all sections, the 3 mW/cm^2 produced significantly more stiffening than the 34 mW/cm^2 and 50 mW/cm^2 conditions ($P \leq .01$). The stiffening from the 9 mW/cm^2 sample significantly differed from that of the 34 mW/cm^2 sample in the anterior ($P \leq .01$) and the 50 mW/cm^2 sample in the anterior ($P \leq .01$) and central ($P \leq .05$). There were no significant differences in stiffening at any section between the 2 most accelerated conditions.

DISCUSSION

In this study, we evaluated the stiffening effects of accelerated corneal CXL protocols. To minimize the control-to-sample variability, 2 disks were punched from each cornea to act as the nonirradiated control and CXL sample, respectively. Keeping a constant energy dose of 5.4 J/cm^2, we performed 4 corneal CXL regimens with varying power and exposure time. To first validate our crosslinking procedures, we compared the resulting stiffness of our crosslinked samples to the respective control samples via stress–strain testing and Brillouin modulus derivation. The 2 techniques consistently showed a significant stiffening effect of CXL for all conditions.

Next, we compared the standard protocol, 3 mW/cm^2 of UVA radiation intensity for 30 minutes of exposure time, with different accelerated protocols. We first used a commonly accepted compression test to compare the stiffening effects of each regimen. The standard CXL protocol, 3 mW/cm^2 of UVA radiation for 30 minutes of exposure time, produced a significantly higher percentage difference in Young's modulus than the 34 mW/cm^2 and 50 mW/cm^2 conditions. The 9 mW/cm^2 condition yielded a significantly higher stiffening effect than the most accelerated protocol. Thus, although the Bunsen-Roscoe law predicts that the crosslinking effects should be similar at a constant energy, our mechanical analysis yielded a radiation intensity/exposure time dependence of stiffening. This is in agreement with previous studies that analyzed accelerated CXL stiffness with compressive mechanical testing. The observed increases in Young's modulus at each irradiance condition, varying from 83% to 18% as a function of radiation power, all fall between the reported values of Wernli et al.[10] and Hammer et al.[11] The consistency between our values and those found in similarly conducted studies further validates our results. However, the studies presented notable differences in the trend between irradiance condition and stiffening effect. Hammer et al.[11] reported a significant decrease in stiffening when the standard 3 mW/cm^2 irradiation condition was compared with 9 mW/cm^2 and 18 mW/cm^2 accelerated protocols. Wernli et al.[10] reported a statistically significant difference in comparing crosslinked samples to their respective controls up until a maximum radiation intensity of 45 mW/cm^2 for 2 minutes of exposure time. However, unlike our findings and those of Hammer et al., the study found a relatively constant effect of CXL from 3 mW/cm^2 through roughly 45 mW/cm^2 before a significant decrease in stiffening magnitude occurred. The differences in results could depend on the variability in experimental procedures. For example, Wernli et al.[10] kept the corneas immersed in a pool of riboflavin solution for 30 minutes before UVA exposure. Our protocol more closely resembled that of Hammer et al.[11] in that riboflavin drops were incrementally applied to the cornea for a total of 30 minutes before radiation exposure. Differing from Hammer et al., our protocol used corneal punches rather than the entire globe. This distinction, by

minimizing the solution runoff from decreasing the sample curvature, might have been responsible for our greater stiffening effects.

The results of the stress–strain testing were also used to validate Brillouin microscopy. We previously determined a log–log linear correlation between Young's modulus and the Brillouin-derived Brillouin modulus.[24] Therefore, our linear correlation between the percentage change in Young's modulus and Brillouin modulus agrees with the previously found relationship.

Using Brillouin microscopy, we were able to expand on our findings as well as those in relevant studies by observing the effects of CXL as a function of depth. This analysis yielded interesting results when comparing the standard protocol (3 mW/cm^2 for 30 minutes) with the slightly accelerated protocol (9 mW/cm^2 for 10 minutes). When the entire cornea was analyzed, the standard condition had a significantly higher Brillouin modulus than the 9 mW/cm^2 protocol. From depth-dependent analysis, the 2 treatments did not show statistically significant differences in anterior stroma but they showed statistically significant differences in the central and posterior portions of the cornea. This suggests the difference between the 2 conditions was primarily the result of the deeper sections. Our findings on depth-dependent stiffening via CXL are in agreement with those of Aldahlawi et al.,[25] who used the resistance to enzymatic degradation properties of CXL corneas to test the effective depth of the procedure. The study similarly showed that up to a maximum radiation power of 18 mW/cm^2 for 5 minutes of exposure time, accelerating the CXL procedure had little effect on the anterior of the corneal stroma but reduced the effective depth of CXL.

It has been suggested that oxygen is a key limiting factor in the CXL process because CXL had no significant stiffening results when performed in a low-oxygen environment.[7] Moreover, oxygen is expected to be consumed in the CXL process because of its transformation into the reactive species that catalyze the covalent bonding of collagen and other matrix proteins in the stroma.[26] Thus, at high-radiation intensity, the rate of oxygen depletion could exceed the rate of oxygen replenishment via diffusion. In particular, the available oxygen concentration is a depth-dependent quantity because it is increasingly difficult for the oxygen to diffuse deeper into the cornea. Therefore, the difference between oxygen depletion and replenishment correlates to both depth and radiation intensity. As a result, when comparing 3 mW/cm^2 and 9 mW/cm^2 conditions for example, it is expected that the anterior portions of the corneas would have similar results while larger stiffening differences should be observed deeper into the corneas. This phenomenon would explain the lower stiffening we observed at the deeper sections of the accelerated cross-linked corneas. However, this effect was primarily seen in the 9 mW/cm^2 condition because the 34 mW/cm^2 and 50 mW/cm^2 conditions significantly lacked stiffening at all 3 sections of the stroma when compared with the standard protocol. The reported anterior lack in stiffening of the most accelerated protocols might be an effect of the measurement technique used. Brittingham et al.,[27] when comparing the standard 3 mW/cm^2 and 9 mW/cm^2 conditions, found a significant decrease in the depth of the demarcation line following accelerated protocols. Therefore, it is possible that for our highest accelerated conditions, the most effected depth of the CXL was too shallow to significantly detect using our Brillouin microscopy parameters. However, a similar threshold of stiffening efficiency was also observed by Wernli et al.[10] It is possible that when the procedure is performed at such a rapid rate, oxygen is unable to diffuse back into the cornea to a significant depth. Past a threshold of a sufficiently oxygenated stroma, we would expect to observe very little stiffening effects of CXL because of the low-oxygen environment, as reported by Richoz et al.[7]

In conclusion, our study confirmed the suboptimum effects of accelerated CXL compared with those of the standard 3 mW/cm^2 condition. Furthermore, using the depth-dependent analysis of Brillouin microscopy, we discovered the lack of CXL stiffening in deeper sections of the cornea, an important difference when comparing the standard methods and accelerated regimens.

WHAT WAS KNOWN

- Accelerated CXL, when compared with the standard 3 mW/cm^2 intensity for 30 minutes regime, provides suboptimum results regarding the stiffening effects on the entire cornea.

WHAT THIS PAPER ADDS

- Brillouin microscopy allowed for a depth-dependent analysis after CXL. The confirmed decrease in effectiveness of accelerated CXL was primarily the result of the lack of stiffening deeper in the cornea compared with what occurs with the standard protocol.

REFERENCES

1. Woodward MA, Randleman JB, Russell B, Lynn MJ, Ward MA, Stulting RD. Visual rehabilitation and outcomes for ectasia after corneal refractive surgery. J Cataract Refract Surg 2008; 34:383–388
2. Rabinowitz YS. Keratoconus. Surv Ophthalmol 1998; 42:297–319. Available at: http://www.keratoconus.com/resources/Major+Review-Keratoconus.pdf. Accessed September 9, 2017
3. Kerautret J, Colin J, Touboul D, Roberts C. Biomechanical characteristics of the ectatic cornea. J Cataract Refract Surg 2008; 34:510–513
4. Wang Z, Chen J, Yang B. Posterior corneal surface topographic changes after laser in situ keratomileusis are related to residual corneal bed thickness. Ophthalmology 1999; 106:406–409; discussion by RK Maloney, 409–410
5. Scarcelli G, Besner S, Pineda R, Kalout P, Yun SH. In vivo biomechanical mapping of normal and keratoconus corneas. JAMA Ophthalmol 2015; 133:480–482. Available at: http://jamanetwork.com/journals/jamaophthalmology/fullarticle/2089674. Accessed September 9, 2017
6. Scarcelli G, Besner S, Pineda R, Yun SH. Biomechanical characterization of keratoconus corneas ex vivo with Brillouin microscopy. Invest Ophthalmol Vis Sci 2014; 55:4490–4495. Available at: http://iovs.arvojournals.org/article.aspx?articleid=2128980. Accessed September 9, 2017
7. Richoz O, Hammer A, Tabibian D, Gatzioufas Z, Hafezi F. The biomechanical effect of corneal collagen cross-linking (CXL) with riboflavin and UV-A is oxygen dependent. Transl Vis Sci Technol 2013; 2:6. Available at: http://www.ncbi.nlm.nih.gov/pmc/articles/PMC3860351/pdf/i2164-2591-2-7-6.pdf. Accessed September 9, 2017

8. Said DG, Elalfy MS, Gatzioufas Z, El-Zakzouk ES, Hassan MA, Saif MY, Zaki AA, Dua HS, Hafezi F. Collagen cross-linking with photoactivated riboflavin (PACK-CXL) for the treatment of advanced infectious keratitis with corneal melting. Ophthalmology 2014; 121:1377–1382
9. Mita M, Waring GO IV, Tomita M. High-irradiance accelerated collagen crosslinking for the treatment of keratoconus: six-month results. J Cataract Refract Surg 2014; 40:1032–1040
10. Wernli J, Schumacher S, Spoerl E, Mrochen M. The efficacy of corneal cross-linking shows a sudden decrease with very high intensity UV light and short treatment time. Invest Ophthalmol Vis Sci 2013; 54:1176–1180. Available at: http://iovs.arvojournals.org/article.aspx?articleid=2127751. Accessed September 9, 2017
11. Hammer A, Richoz O, Arba Mosquera S, Tabibian D, Hoogewoud F, Hafezi F. Corneal biomechanical properties at different corneal cross-linking (CXL) irradiances. Invest Ophthalmol Vis Sci 2014; 55:2881–2884. Available at: http://iovs.arvojournals.org/article.aspx?articleid=2128027. Accessed September 9, 2017
12. Chai D, Gaster RN, Roizenblatt R, Juhasz T, Brown DJ, Jester JV. Quantitative assessment of UVA-riboflavin corneal cross-linking using nonlinear optical microscopy. Invest Ophthalmol Vis Sci 2011; 52:4231–4238. Available at: http://iovs.arvojournals.org/article.aspx?articleid=2187552. Accessed September 9, 2017
13. Kymionis GD, Tsoulnaras KI, Grentzelos MA, Liakopoulos DA, Tsakalis NG, Blazaki SV, Paraskevopoulos TA, Tsilimbaris MK. Evaluation of corneal stromal demarcation line depth following standard and a modified-accelerated collagen cross-linking protocol. Am J Ophthalmol 2014; 158:671–675
14. Scarcelli G, Polacheck WJ, Nia HT, Patel K, Grodzinsky AJ, Kamm RD, Yun SH. Noncontact three-dimensional mapping of intracellular hydromechanical properties by Brillouin microscopy. Nat Methods 2015; 12:1132–1134. Available at: https://www.ncbi.nlm.nih.gov/pmc/articles/PMC4666809/pdf/nihms722557.pdf. Accessed September 9, 2017
15. Scarcelli G, Yun SH. Confocal Brillouin microscopy for three-dimensional mechanical imaging. Nat Photonics 2007; 9:39–43. Available at: http://www.ncbi.nlm.nih.gov/pmc/articles/PMC2757783/pdf/nihms145085.pdf. Accessed September 9, 2017
16. Scarcelli G, Yun SH. Multistage VIPA etalons for high-extinction parallel Brillouin spectroscopy. Opt Express 2011; 19:10913–10922. Available at: https://www.ncbi.nlm.nih.gov/pmc/articles/PMC3482891/pdf/oe-19-11-10913.pdf. Accessed September 9, 2017
17. Berghaus KV, Yun SH, Scarcelli G. High speed sub-GHz spectrometer for Brillouin scattering analysis. J Vis Exp 2015; e53468. Available at: https://www.ncbi.nlm.nih.gov/pmc/articles/PMC4758767/pdf/nihms761634.pdf
18. He X, Liu J. A quantitative ultrasonic spectroscopy method for noninvasive determination of corneal biomechanical properties. Invest Ophthalmol Vis Sci 2009; 50:5148–5154. Available at: http://iovs.arvojournals.org/article.aspx?articleid=2164751. Accessed September 9, 2017
19. Kikkawa Y, Hirayama K. Uneven swelling of the corneal stroma. Invest Ophthalmol 1970; 9:735–741. Available at: http://iovs.arvojournals.org/article.aspx?articleid=2203463. Accessed September 9, 2017
20. Wilson G, O'Leary DJ, Vaughan W. Differential swelling in compartments of the corneal stroma. Invest Ophthalmol Vis Sci 1984; 25:1105–1108. Available at: http://iovs.arvojournals.org/article.aspx?articleid=2176951. Accessed September 9, 2017
21. Ortiz S, Siedlecki D, Grulkowski I, Remon L, Pascual D, Wojtkowski M, Marcos S. Optical distortion correction in optical coherence tomography for quantitative ocular anterior segment by three-dimensional imaging. Opt Express 2010; 18:2782–2796. Available at: http://www.opticsinfobase.org/abstract.cfm?uri=oe-18-3-2782. Accessed September 9, 2017
22. Scarcelli G, Kling S, Quijano E, Pineda R, Marcos S, Yun SH. Brillouin microscopy of collagen crosslinking: Noncontact depth-dependent analysis of corneal elastic modulus. Invest Ophthalmol Vis Sci 2013; 54:1418–1425. Available at: http://iovs.arvojournals.org/article.aspx?articleid=2128290. Accessed September 9, 2017
23. Scarcelli G, Pineda R, Yun SH. Brillouin optical microscopy for corneal biomechanics. Invest Ophthalmol Vis Sci 2012; 53:185–190. Available at: http://iovs.arvojournals.org/article.aspx?articleid=2126760. Accessed September 9, 2017
24. Scarcelli G, Kim P, Yun SH. In vivo measurement of age-related stiffening in the crystalline lens by Brillouin optical microscopy. Biophys J 2011; 101:1539–1545. Available at: http://www.cell.com/biophysj/pdf/S0006-3495(11)00950-7.pdf. Accessed September 9, 2017
25. Aldahlawi NH, Hayes S, O'Brart DPS, Meek KM. Standard versus accelerated riboflavin–ultraviolet corneal collagen crosslinking: resistance against enzymatic digestion. J Cataract Refract Surg 2015; 41:1989–1996. Available at: http://www.jcrsjournal.org/article/S0886-3350(15)01065-2/pdf. Accessed September 9, 2017
26. McCall AS, Kraft S, Edelhauser HF, Kidder GW, Lundquist RR, Bradshaw HE, Dedeic Z, Dionne MJC, Clement EM, Conrad GW. Mechanisms of corneal tissue cross-linking in response to treatment with topical riboflavin and long-wavelength ultraviolet radiation (UVA). Invest Ophthalmol Vis Sci 2010; 51:129–138. Available at: http://iovs.arvojournals.org/article.aspx?articleid=2185576. Accessed September 9, 2017
27. Brittingham S, Tappeiner C, Frueh BE. Corneal cross-linking in keratoconus using the standard and rapid treatment protocol: differences in demarcation line and 12-month outcomes. Invest Ophthalmol Vis Sci 2014; 55:8371–8376. Available at: http://iovs.arvojournals.org/article.aspx?articleid=2212704. Accessed September 9, 2017

Disclosure: *None of the authors has a financial or proprietary interest in any material or method mentioned.*